Synthesis and Physical Characterization of Novel Heme-Based Model Systems for Photoinitiated Electron Transfer. 2. Direct Ruthenation of Microperoxidase-11†

B. Fan,‡ M. C. Simpson,§ J. A. Shelnutt,§ L. Martinez,‡ R. Falcon,‡ T. Buranda,‡ A. J. Pastuszyn,|| and M. R. Ondrias*,‡

Departments of Chemistry and Biochemistry, University of New Mexico, Albuquerque, New Mexico 87131, and Fuel Sciences Divison, Sandia National Laboratory, Albuquerque, New Mexico 87185

Received January 15, 1997⊗

This paper describes the design, synthesis, and initial characterization of a second type of model electron transfer system based upon microperoxidase-11 (MP-11) that differs significantly from those described in the preceding article. In this system, a photoactive ruthenium tris(bipyridyl) donor is covalently attached directly to MP-11. Peptide digestion followed by chromatographic analysis was used to establish that the ruthenium moiety bonds to the lysine residue of the MP-11 peptide. This arrangement eliminates complications arising from the equilibrium complexation of ruthenium donor and heme acceptor required for the model systems described in the previous article and leaves an axial position in the octahedral geometry of the heme iron open for ligation. Various optical spectroscopies and molecular modeling calculations were employed to characterize the equilibrium properties and interchromophore interactions of RuMP-11. Preliminary luminescence-quenching, transient absorption, and transient resonance Raman studies demonstrated that rapid reversible electron transfer can be photoinitiated in this system.

Introduction

The long-range outer-sphere electron transfer exhibited by many protein systems differs in fundamental ways from the faster inner-sphere processes of smaller inorganic systems.[1,2] The most important of these are the potential roles played by the protein matrix itself in modulating the structures of redox-active prosthetic groups and directly regulating the kinetics of electron transfer. The mechanisms by which protein structure modulates ET rates is a subject of continuing debate and inquiry. The results of recent experimental studies of photoinduced ET in ruthenium-derivatized cytochromes have revealed the complexity of the problem.[3] These studies suggest that, in some cases, the protein functions as a nonspecific dielectric solvent,[4] while in others, the specific identities of amino acids in the putative ET pathways can significantly influence the observed kinetics.[5]

In view of the complexity of protein systems, there is a clear need for simpler yet relevant model systems for heme protein electron transfer and more direct probes of molecular structural dynamics at protein active sites during electron transfer. Time-resolved spectroscopies have been utilized to probe the dynamics of photoinduced electron transfer in ruthenated heme proteins.[6] Initial transient resonance Raman studies of ruthenated cytochromes *c* have yielded promising data concerning the structural dynamics at the heme that must accompany electron transfer.[7] However, similar studies of carefully designed model systems are required for an unambiguous interpretation of the transient spectra.

In this work, a new approach has been developed to covalently attach a ruthenium tris(bipyridyl) group to the amino groups of microperoxidases and thus produce unique ET model systems. Here we describe our initial synthesis and characterization of the equilibrium and photophysical properties of ruthenated microperoxidase-11 (RuMP-11). Rapid electron transfer from photoexcited $Ru(bpy)_3^{2+}$* to the ferric heme of MP-11 was observed by different time-resolved spectroscopic methods. These observations demonstrate that directly ruthenated MPs are a promising series of model systems with which to address many fundamental aspects of biological ET processes.

Materials and Methods

Microperoxidase-11 (MP-11) was purchased from Sigma and used without further purification. The synthesis of the reactive precursor, hydroxysuccinimide ester of bis(2,2′-bipyridine)(4′-methyl-2,2′-bipyridine-4-carboxylic acid)ruthenium(II), RuOSu, was performed by using a procedure of Peek et al. with minor modifications.[8]

* To whom correspondence should be addressed.

† Abbreviations used: ET, electron transfer; EnT, energy transfer; RR, resonance Raman; MP-11, microperoxidase-11 (heme undecapeptide); RuMP-11, microperoxidase-11 covalently attached to a derivatized $Ru(bpy)_3$ as described in the text; acMP-11, microperoxidase acetylated at both amino groups as described in the preceding article; Im, imidazole.

‡ Department of Chemistry, University of New Mexico.

§ Sandia National Laboratory.

|| Department of Biochemistry, University of New Mexico.

⊗ Abstract published in *Advance ACS Abstracts,* August 1, 1997.

(1) Orman, L. K.; Anderson, D. R.; Yabe, T.; Hopkins, J. B. in *Electron Transfer in Biology and the Solid State*; Johnson, M. K., et al., Eds.; American Chemical Society: Washington, DC, 1990.

(2) Marcus, R. A.; Sutin, N. *Biochim. Biophys. Acta* **1985**, *811*, 265.

(3) (a) Gray, H. B.; Winkler, J. R. *Pure Appl. Chem.* **1992**, *64*, 1257. (b) Winkler, J. R.; Gray, H. B. *Chem. Rev.* **1992**, *92*, 369. (c) Bjerrum, M. J.; Casimiro, D. R.; Wuttke, D. S. *J. Bioenerg. Biomembr.* **1995**, *27*, 295.

(4) Bowler, B. E.; Meade, T. J.; Mayo, S. L.; Richards, J. H.; Gray, H. B. *J. Am. Chem. Soc.* **1989**, *111*, 8757.

(5) (a) Beratan, D. N.; Betts, J. N.; Onuchic, J. N. *Science* **1991**, *252*, 1285. (b) Onuchic, J. N.; Beratan, D. N.; Winkler, J. R. *Annu. Rev. Biophys. Biomol. Struct.* **1992**, *21*, 349.

(6) (a) Winkler, J. R.; Malmstrom, B. G.; Gray, H. B. *Biophys. Chem.* **1995**, *54*, 199. (b) Geren, L. M.; Beasley, J. R.; Fine, B. R.; Saunders, A. J.; Hibdon, S.; Pielak, G. J.; Durham, B.; Millett, F. *J. Biol. Chem.* **1995**, *270*, 2466.

(7) (a) Simpson, M. C.; Millett, F.; Fan, B.; Ondrias, M. R. *J. Am. Chem. Soc.* **1995**, *117*, 3296. (b) Simpson, M. C.; Millett, F.; Pan, L. P.; Larsen, R. W.; Hobbs, J. D.; Fan, B.; Ondrias, M. R. *Biochemistry* **1996**, *35*, 10019.

(8) Peek, B. M.; Ross, G. T.; Edwards, S. W.; Meyer, G. J.; Meyer, T. J.; Erickson, B. W. *Int. J. Pept. Protein Res.* **1991**, *38*, 114.

S0020-1669(97)00040-2 CCC: $14.00

MP-11 was covalently ruthenated as follows: A 10 mg sample of MP-11 was dissolved in 500 μL of 50 mM $NaHCO_3$ and mixed with 10 mg of RuOSu dissolved in 200 μL of DMF. The mixture was stirred in the dark for 4 h at room temperature and then separated with a 1 × 60 cm Bio-Gel p-2 (Bio-Rad) column eluted with 100 mM pH 7.0 sodium phosphate buffer. The crude product was further purified by HPLC on a C18 column using 0.1% TFA and a gradient of 5−60% acetonitrile. The elution fractions were monitored at 287 and 397 nm simultaneously. The fractions with significant absorbance at both of the wavelengths were collected as product.

The modification site was confirmed by trypsin digestion. The product was incubated in sodium bicarbonate buffer at pH 8.0 with a 1:100 trypsin:sample ratio. Another sample was prepared with exactly the same composition except that no trypsin was added. Both the samples were incubated for 2 h at 37 °C and then separated with HPLC on a C18 column. The same procedure was performed on MP-11 as a control.

Electrospray ionization mass spectra were obtained using a Vestec electrospray source and a Model 201 single-quadrupole mass spectrometer (Vestec, Houston, TX) fitted with an *m*/*z* 200 range. Samples were delivered to the source in a 10 μL injection loop at 5 μL/min in a 4% acetic acid:50% acetonitrile, by weight, solution.

UV−vis absorption spectra were obtained with an HP8452A diode array spectrometer, and static luminescence was measured with a Perkin-Elmer PL-5 fluorometer. Resonance Raman experiments were performed with a Chromex 500IS monochromator equipped with a Princeton Instrument CCD detector operating at −100 °C. The signal was collected with a conventional backscattering geometry. A polarization scrambler was used to remove the polarization bias of the optics. Excitation was provided by a hydrogen Raman shift cell pumped by the third harmonic of a Quanta-Ray DCR-II YAG laser (see figure captions for additional details). Broad-band transient absorption spectra were collected using instrumentation described, in detail, elsewhere.[9] Briefly, the output from the Nd:YAG laser based system was used as the pump and a 75 W xenon flashlamp (Photon Technologies International) was used as the probe. The probe beam was focused into the middle of the sample holder where it was crossed with the pump beam. The transmitted probe beam was focused onto a slit of a Spex Triplemate spectrograph coupled to a gated EG&G Princeton Applied Research 1420 diode array detector equipped with a 1461 controller interfaced with a computer. Typically for each absorption profile, intensities were measured for the background, the ground state (probe only), the excited state (pump/probe), and the pump only. The background and pump-only data sets were used for dark and emission or scattered laser light corrections, respectively. Time resolution was achieved by using an optically triggered PAR 1304 gated pulse amplifier.

Computer modeling of the minimum-energy structure of RuMP-11 was accomplished via protocols described in the preceding article.

Results and Discussion

Synthesis. MP-11 was ruthenated by reacting it with derivatized $Ru(bpy)_3^{2+}$ having a single 4-methyl-4′-carboxbipyridine in a manner analogous to that described in the previous article. The reaction mixture was then separated and purified by sequencial use of gel filtration and HPLC. The eluent was monitored at two different wavelengths, 287 and 398 nm, corresponding to isolated $Ru(bpy)_3^{2+}$ absorption and isolated MP-11 absorption, respectively. Fractions exhibiting absorbance at both wavelengths were considered to be the ruthenated product, while those having absorbance at only one wavelength were considered to be the unreacted starting materials. Under the experimental conditions, polymerization occurred, but the polymer was not further characterized. The polymeric product lowered the overall yield dramatically, leading to a final yield of ∼60% for the desired product.

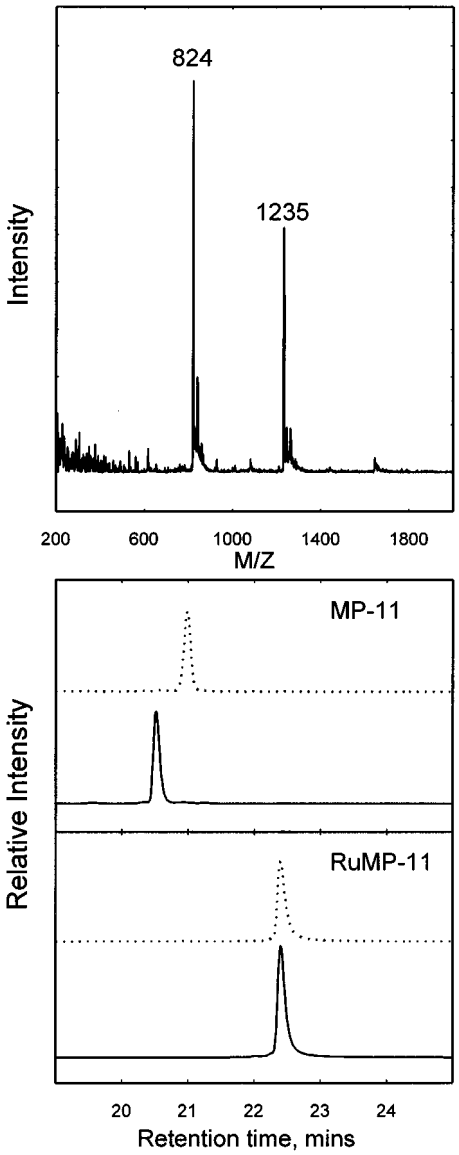

Figure 1. Characterization of the chemical structure of RuMP-11. Bottom: Chromatograph of the trypsin digestion experiments: upper panel, MP-11; lower panel, RuMP-11. In both cases, the dotted line represents the sample without trypsin and the solid line represents the sample with trypsin. Samples were loaded as aqueous solutions and eluted with a 0.1% TFA solution and a gradient of 5−60% acetonitrile. Top: Electrospray mass spectrum of RuMP-11. See text for experimental details.

Electrospray mass spectra of RuMP-11 (Figure 1) show the expected molecular ion peaks based on the following analysis. The iron heme is taken to be *m*/*z* 617, the undecapeptide *m*/*z* 1226, and the $[(2,2'\text{-bipyridine})_2(4'\text{-methyl-}2,2'\text{-bipyridine-}4\text{-carboxylic acid})Ru^{II}]^{2+}$ *m*/*z* 628. Thus the molecular weight was calculated to be 2471 for RuMP-11. Since RuMP-11 bears three net nonproton positive charges contributed by the Ru^{2+} and the heme, *m*/*z* values can be interpreted according to $m/z = [M - n]/[3 - n]$, where *M* is the molecular weight and *n* is the deprotonation number. In the case of RuMP-11, the doubly and triply charged species appear at *m*/*z* 1235 and 824, corresponding to molecular weights of 2471 and 2472, respectively.

Two possible modification sites (the N-terminal amino group and the lysine side chain amino group) exist even after the molecular weight is confirmed. The selectivity of the modification toward an ϵ- or α-amino acid can be controlled by the use of different solution conditions which exploit the differences in amino group pK_b values and the kinetics of the ruthenation

(9) Buranda, T.; Larsen, R. W.; Niu, S.; Ondrias, M. R. *J. Phys. Chem.* **1996**, *100*, 18868.

reaction. Since the lysine ϵ-amino group has the lower pK_b value, it reacts faster than the N-terminal amino group under the same conditions; thus a lower pH (8.5) and a smaller concentration of ruthenium reagent were used to favor lysine modification of MP-11. HPLC showed that only one major peak absorbed at both 287 and 397 nm. No effort was made to isolate the N-terminal modified species.

The exact position of modification was verified by enzymatic digestion methods using trypsin, an enzyme which cleaves peptides after lysine residues. Figure 1 shows the results of the HPLC separation of untreated RuMP-11 and free MP-11. In the case of free MP-11, the retention time of the intact MP-11 peak is 21.1 min, while that of the digested MP-11 is 20.6 min; the shorter retention time indicates the digestion of the Val-Glu-Lys oligomer from MP-11 to form MP-8. The same procedure was performed with the ruthenated product. No difference in the retention time between the "digested" and intact RuMP-11 was observed, confirming that the lysine residue of RuMP-11 is protected from digestion and is, in fact, the sole site of ruthenation under the experimental conditions.

Bis(2,2′-bipyridine)(2,2′-bipyridine-4,4′-dicarboxylic acid)-ruthenium(II) was previously attached to horse heart cytochrome *c* using a two-step procedure.[10] First, one of the carboxylic groups of the 4,4′-dicarboxybipyridine ligand was deprotonated using a titration of sodium hydroxide solution to prevent the formation of an ester. The remaining carboxylic group was activated by converting it to a succinyl ester, the activated ligand was then incubated with cytochrome *c*. Thus, the first step yielded a ligand-modified product. After separation, the products were incubated with excess $Ru(bpy)_2CO_3$ to yield the final products. There are several drawbacks to this procedure: (1) The pH titration is an ineffective way to deactivate the carboxylic group because of the equilibrium nature of pH titration. (2) The two-step procedure requires more total incubation time and thus increases the possibility of denaturation of the protein. This may not be a great problem for a relatively stable protein like cytochrome *c*, but it severely limits the general application of the procedure for protein modification. (3) The existence of the extra negative charge on the bipyridine may cause complications in interprotein interactions, especially for positively charged enzymes.

All of these drawbacks are overcome or improved by the one-step approach used in the present study. A similar procedure was recently used for cytochrome *c* modification by Millett and co-workers[11] and has proved to be quite versatile as a general method for protein amino group modification. Since only one of the methyl groups was transformed into a carboxyl group, the complications introduced by the free carboxyl group after modification are eliminated. Also, the procedure requires only a single-step reaction involving the target substrate, greatly reducing the time that the enzyme is exposed to nonphysiological conditions.

Equilibrium and Spectroscopic Properties of RuMP-11. Aggregation of MPs results largely from a combination of hydrophobic interactions and intermolecular ligation and changes the heme iron spin state.[12] This transition is quite evident in both the aborption and the resonance Raman spectra of MP-11 (see previous article). Aggregation can be greatly decreased by protecting the amino groups and thus eliminating the potential for intermolecular ligation.[12] In the case of procedures described above, only one of the two amino groups of MP-11 (lysine) was used for the ruthenation, leaving the N-terminus amino group free and potentially available for intermolecular coordination. Evidence for the lysine amino group participation in the aggregation process is apparent in the visible region of the absorption spectra of RuMP-11(Figure 2). The weak peak at 620 nm is assigned as a porphyrin to Fe(III) charge transfer band or a mixture of a charge transfer band and the α/β band.[13] Even though its exact assignment is still controversial, this band is characteristic of ferric high-spin heme species. The intensity of the 640 nm band increases in going from free MP-11 to RuMP-11(data not shown), indicating a decrease in intermolecular aggregation. The same type of behavior is observed following acetylation of MP-11 (see previous article); however, the magnitudes of the spectral changes are considerably larger. This strongly suggests that both the lysine and the terminal amino groups can participate in the aggregation process. Thus, aggregation may still be a factor in the RuMP-11 system. This is indeed the case, as can be seen in the shift of the absorption maximum at 396 nm for acMP-11 to 404 nm for RuMP-11.

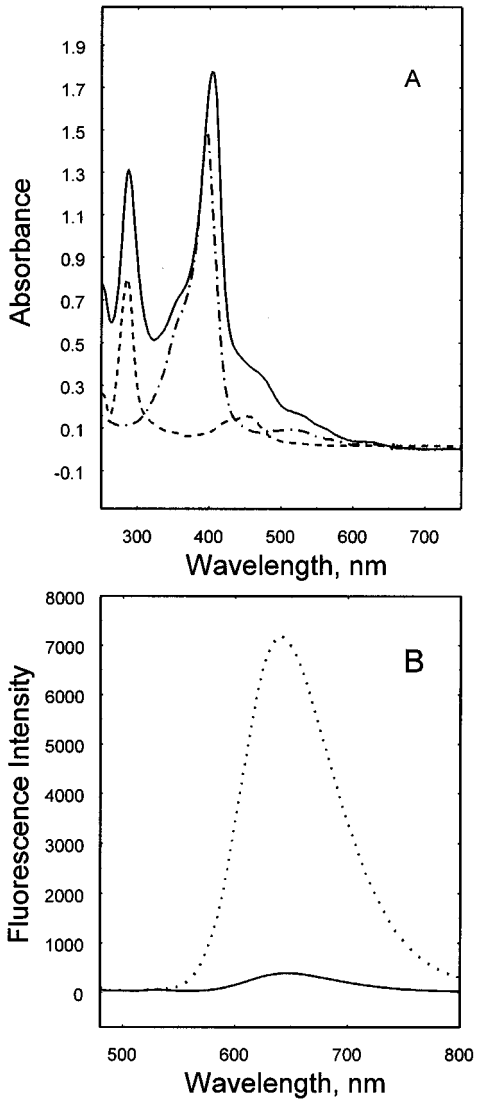

Figure 2. Panel A: UV−vis absorption spectra of $Ru(bpy)_3Cl_2$ (dashed line), acMP-11 (dot-dashed line), and RuMP-11 (solid line). Panel B: Emission spectra of RuMP-11 (solid line) and RuProHis dipeptide (dotted line). All samples were ~10 μM in 100 mM phosphate buffer at pH 7.0. Luminescence spectra were obtained using 450 nm excitation.

(10) Pan, L. P.; Durham, B.; Wolinska, J.; Millett, F. *Biochemistry* **1988**, *27*, 7180.
(11) Liu, R. Q.; Geren, L.; Anderson, P.; Peffer, N.; Farris, J. L.; McKee, A.; Durham, B.; Millett, F. *Biochimie* **1995**, *75*, 549.
(12) (a) Urry, D. W. *J. Am. Chem. Soc.* **1967**, *89*, 4190. (b) Wang, J. S.; Van Wart, H. E. *J. Phys. Chem.* **1989**, *93*, 7925.
(13) Makinen, M. W.; Churg, A. K. In *Iron Porphyrins*; Lever, A. B. P., Gray, H. B., Eds.; Addison-Wesley: Amsterdam, 1983; Part 1.

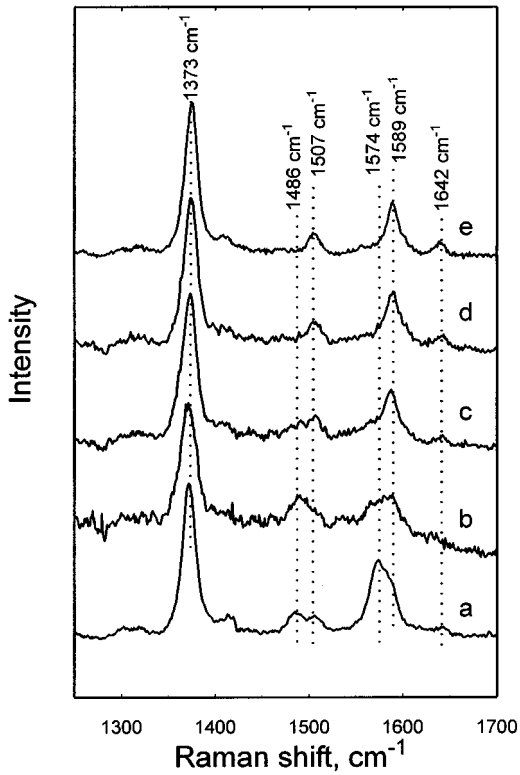

Figure 3. Resonance Raman spectra of different heme species: (a) acetylated MP-11; (b) RuMP-11; (c) RuMP-11/imidazole complex; (d) free MP-11; and (e) acMP-11/imidazole complex. Spectra were taken using 416 nm excitation (0.075 mJ/pulse). All samples were 100 μM microperoxidase species (and 100 mM imidazole where appropriate) in 100 mM phosphate buffer at pH 7.0.

For this reason, the initial electron transfer studies described later were conducted with the imidazole-bound RuMP-11 species which displays no indications of aggregation.

Absorption spectra are sensitive to interchromophore interactions. The close similarity between the RuMP-11 spectrum and the weighted sum of RuProHis and acMP-11 spectra demonstrates that no significant dipole−dipole interactions exist between the two chromophores. Curve fits of the LC $\pi-\pi^*$ bands at 288 nm do show a small broadening (∼10%) of this band for RuMP-11. In contrast to the absorption results, the luminescence behavior of the $Ru(bpy)_3^{2+}$ group is markedly altered by covalent attachment to the heme, indicating interaction between the excited states of the two chromophores. For comparison, the emission spectrum of RuProHis is also included in Figure 2. The luminescence maximum shifts from 641 nm for the RuProHis to 648 nm for RuMP-11. The luminescence intensity of the $Ru(bpy)_3^{2+}$ moiety of RuMP-11 is also diminished by approximately an order of magnitude compared to that of the Ru $(bpy)_3^{2+}$−Pro group of the RuProHis peptide. Since the chemical natures of the bipyridine ring substituents are identical in the two species, it is almost certain that strong luminescence quenching occurs via the heme of MP-11.

The aggregation behavior of RuMP-11 can be further monitored by resonance Raman experiments. The heme Raman modes ν_3 and ν_2 are particularly sensitive to spin state and/or ligation states. Resonance Raman spectra of acMP-11, RuMP-11, the RuMP-11/imidazole complex, MP-11, and the acMP-11/imidazole complex are shown in Figure 3. The major differences among these species occur in the spin-state-sensitive lines, ν_2 and ν_3. In spectra of low-spin ferric hemes, these modes occur at ∼1505 and 1590 cm^{-1}, respectively. The core expansion exhibited by high-spin hemes causes these modes to downshift to ∼1485 and ∼1575 cm^{-1}.

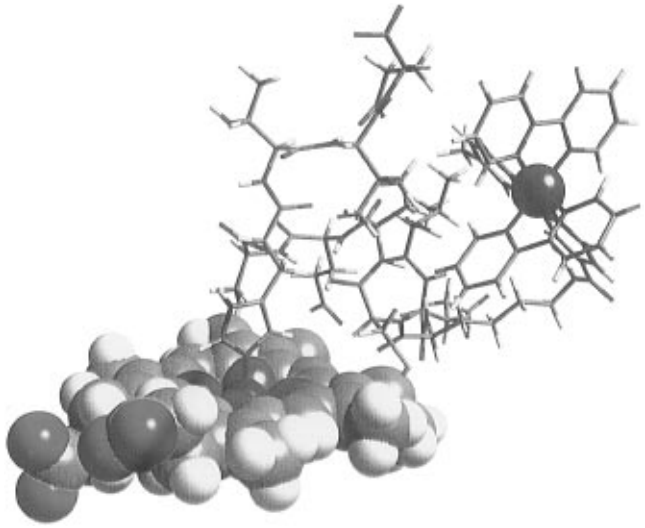

Figure 4. Computer-energy-minimized structure of RuMP-11. See text for details.

The hemes of both acMP-11 and RuMP-11 exist in solution as mixtures of different spin states, characterized by the coexistence of high-spin and low-spin bands for ν_3 (1486 and 1507 cm^{-1}) and ν_2 (1574 and 1589 cm^{-1}) in their resonance Raman spectra (traces a and b in Figure 3). Due to the overlap of a band from $Ru(bpy)_3^{2+}$−Lys group at 1492 cm^{-1} with ν_3, quantification of the behavior of this band in RuMP-11 is impossible. However, a comparison of the relative magnitudes of the two ν_2 components reveals that the intensity of the 1574 cm^{-1} (high-spin) band is much higher than that of the 1589 cm^{-1} (low-spin) band for acMP-11, while, for RuMP-11, the proportion of low-spin heme is larger. In fact, the 1574/1589 intensity ratio for RuMP-11 lies between that of acMP-11 and unprotected MP-11 (trace d). This indicates a substantial population of low-spin heme species in the RuMP-11 sample and, by inference, the existence of some aggregation due to the partial ligation of the heme with the unprotected N-terminus amino groups.

RuMP-11 readily binds imidizole and other strong-field ligands. The addition of 10 mM imidazole to a 10 μM solution of RuMP-11 produces an absorption spectrum characteristic of a completely low-spin (six-coordinate) heme (data not shown). While the existence of some aggregated (low-spin) heme in the initial RuMP-11 sample makes exact quantification of an association constant difficult, it can be estimated as greater than 5×10^3 M^{-1}. Complexation between the RuMp-11 and imidazole was also examined with resonance Raman spectroscopy. The RuMP-11/imidazole complex (trace c) exhibits only the spectral features of a low-spin heme, confirming that it readily forms six-coordinate adducts with external ligands. In this regard, RuMP-11 mirrors the behavior (except for the additional $Ru(bpy)_3^{2+}$ band at ∼1485 cm^{-1}) of acMP-11 (trace e), indicating that attachment of the ruthenium group leaves the heme coordination site open for external ligation.

Computer Modeling. The RuMP-11 system has the added advantage of being small enough to be accurately modeled using available molecular mechanics protocols. The energy-minimized structure of ruthenated MP-11 obtained using a force field developed explicitly for metalloporphyrin geometries by Shelnutt and co-workers[14] is shown in Figure 4, and a summary

(14) (a) Jentzen, W.; Simpson, M. C.; Hobbs, J. D.; Song, X.; Shelnutt, J. A. *J. Am. Chem. Soc.* **1995**, *117*, 11085. (b) Sparks, L. D.; Medforth, C. J.; Park M.-S.; Ondrias, M. R.; Shelnutt, J. A. *J. Am. Chem. Soc.* **1993**, *115*, 581.

Table 1. Energetic and Structural Parameters of Computer-Simulated $Ru(bpy)_3^{2+}$, acMP-11, Im, RuMP-11, and Its Imidazole Complex[a]

	$Ru(bpy)_3^{2+}$	acMP-11	RuMP-11	Im	RuMP-11/Im	$\Delta E_{complex}$[b]
total energy	91.98	228.25	315.95	15.32	327.45	−3.82
bonds	9.47	20.84	30.66	10.03	30.90	−9.79
angles	19.26	142.4	161.58	5.25	177.87	11.04
torsion	0.20	33.09	31.87	0	32.32	0.45
inversion	0	1.86	1.71	0	1.77	0.06
van der Waals	62.99	80.68	146.43	0.02	141.01	−5.44
electrostatics	0.04	−1.18	−0.31	0.02	−0.40	−0.11
H-bonds	0	−49.43	−55.99	0	−56.02	−0.03
R_{Ru-Fe}, Å, through-space			20.42		19.39	
R_{Ru-Fe}, Å, through-bond			32.37		32.37	
$R_{edge-edge}$,[c] Å, through-space			12.22		12.07	

[a] All structures are minimized at a dielectric constant of 79*r*; all energies are in kcal/mol. [b] $\Delta E = E_{total}$[complex] − {E_{total}[RuMP-11] + E_{total}[imidazole]}. [c] $R_{edge-edge}$ is the closest contact distance between the heme and the $Ru(bpy)_3^{2+}$ group.

of the energetics of RuMP-11 vs isolated $Ru(bpy)_3^{2+}$ plus MP-11 is given in Table 1. During the modeling procedures, care was exercised to ensure that the final structure represents a reasonable energetic minimum using techniques described in the previous article.

While the attachment of the derivatized $Ru(bpy)_3^{2+}$ group to MP-11 increases the van der Waals energy of RuMP-11 relative to the isolated species, it produces no large-scale distortions of either moiety. The energy-minimized structure places the Ru group far from the heme, thus producing a longer through-space donor/acceptor electron transfer distance than that calculated for the acMP-11/RuProHis system of the previous article (in addition to the required longer through-bond distance).

The sixth coordination site of the heme is quite exposed to solvent in the minimized structure, allowing imidazole to bind without significant perturbation of the RuMP-11 structure. In particular, ligand binding produces only small changes in donor/acceptor distance. The predicted exothermicity of the reaction (∼3.8 kcal/mol) is consistent with the experimentally observed tight binding of the Im/RuMP-11 complex.

Photodynamics. The luminescence quantum yield is a measure of the ratio of radiative and nonradiative decay rates of a given excited state. The strong quenching of $Ru(bpy)_3^{2+}$ luminescence in the RuMP systems demonstrates that alternative nonradiative deactivation pathways exist for photoexcited $Ru(bpy)_3^{2+}$*. Since the RuProHis luminescence (see previous article) is much more intense than that of RuMPs, it must be assumed that $Ru(bpy)_3^{2+}$/heme interactions rather than the chemical derivatization of $Ru(bpy)_3^{2+}$ are responsible for the quenching of the RuMP-11 luminescence. The two most likely mechanisms for quenching are electron transfer (ET) or energy transfer (EnT).

Energy transfer occurs via through-space dipolar interactions between D* and A. These can be operative to many tens of angstroms under the right circumstances. Efficient EnT depends on several factors as described in the theoretical treatment first derived by Förster:[15] One of the major requirements for efficient EnT is a good spectral overlap between donor emission and acceptor absorption spectra. This is clear from the dependence of the rate constant on the donor emission ($f_D(\lambda)$) and acceptor absorption ($\epsilon_A(\lambda)$) overlap integral ($J = \int \epsilon_A(\lambda)\, f_D(\lambda)\, \lambda^4\, d\lambda$). In the case of RuMP systems, the donor emission does not overlap with the acceptor absorption because only minimal heme absorption exists around 650 nm. This lack of spectral overlap, coupled with the resonance Raman and transient absorption evidence discussed below, makes it extremely unlikely that EnT plays a significant role in the photodynamics of the RuMP-11.

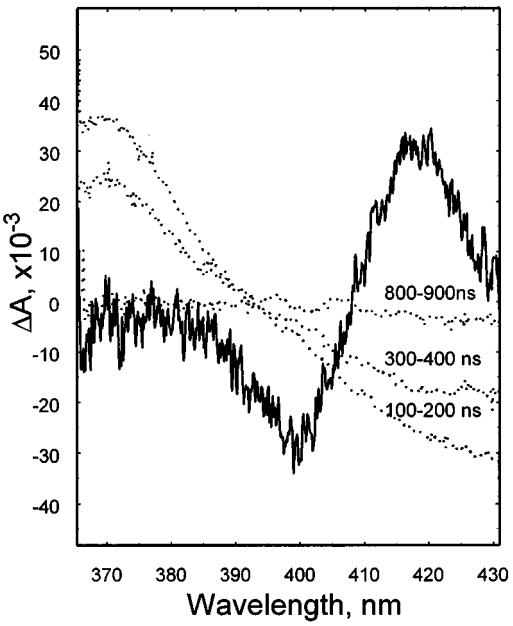

Figure 5. Transient absorption spectrum of RuMP-11 obtained between 100 and 200 ns after 532 nm excitation. The dotted lines are the transient absorptions of free $Ru(bpy)_3^{2+}$ at different time scales. The sample was 50 μM RuMP-11 in 100 mM phoshate buffer at pH 7.0.

While the excited state energetics of the Ru* donor/heme acceptor pair argue against an EnT quenching mechanism, the thermodynamics involved in the electron transfer processes of this pair are quite favorable. An examination of the reduction potentials of $Ru^{II}bpy^*$ ($E^\circ_{Ru^{II*}/Ru^{III}} = -0.86$ V)[16] and the microperoxidase heme ($E^\circ_{Fe^{III}/Fe^{II}} = -0.27$ V)[17] reveals that ET is a thermodynamically favored reaction.

Photophysical Behavior of RuMP-11. The primary evidence for an electron transfer quenching mechanism of the ruthenium excited state is the behavior of the broad-band transient difference absorption spectrum of MP-11 in the 100−200 ns range. Figure 5 offers a comparison of transient absorption spectra obtained from free $Ru(bpy)_3^{2+}$ and RuMP-11 under the same experimental conditions. These data are consistent with the strong quenching of $Ru(bpy)_3^{2+}$ and clearly demonstrate that the transient spectrum created within 200 ns of photoexcitation of RuMP-11 does not arise from the $Ru(bpy)_3^{2+}$* moiety. Instead, the behavior of RuMP-11 upon laser excitation is consistent with the production of a ferrous heme, indicated by the transient peak at 416 nm and trough at 400 nm. This transient absorption behavior in the Soret region clearly indicates heme photoreduction and thus

(15) For a concise description of EnT, see: Cantor, C. R.; Schimmel, P. R. *Biophysical Chemistry*; Freeman: San Francisco, CA, 1980; Part II.

(16) Karvarnos, G. J.; Turro, N. J. *Chem. Rev.* **1986**, *86*, 401.
(17) Loach, P. A.; Harbury, H. A. *J. Biol. Chem.* **1960**, *235*, 3640.

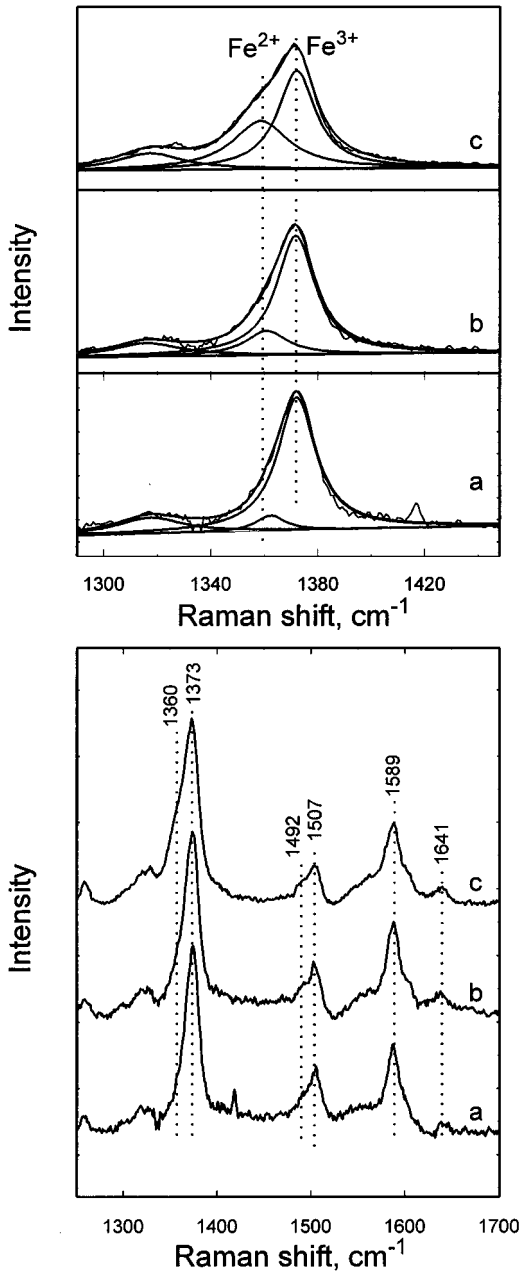

Figure 6. Transient resonance Raman spectra of RuMP-11/imidazole complex under anerobic conditions: (a) low power (0.075 mJ/pulse); (b) medium power (0.18 mJ/pulse); (c) high power (0.75 mJ/pulse). The bottom panel depicts the response of the entire high-frequency region of the spectrum to increasing laser power. The top panel shows the behavior of ν_4 in more detail. Curve-fitting protocols were the same as in Figure 5 of the preceding article. Samples were 100 μM RuMP-11 and 100 mM imidazole in 100 mM phosphate buffer at pH 7.0; 416 nm pulses of 10 ns duration and 10 Hz repetition rate were used for excitation.

supports an electron transfer mechanism for the luminescence quenching. Unfortunately, instrumental limitations restrict the scope of the time-resolved studies and faster time resolution is needed for further investigation.

Transient resonance Raman data also show definitive evidence for electron transfer between the ruthenium excited state and the microperoxidase ferric heme (Figure 6). In the spectra of both RuMP-11 (data not shown) and its imidazole complex, clear evidence for heme reduction was observed within 10 ns of laser excitation, indicated by the power-dependent growth of the Raman bands around 1360 cm^{-1} (ferrous ν_4). This heme reduction must occur through ET from the covalently attached $Ru(bpy)_3^{2+}$ derivative since no photoreduction of heme was

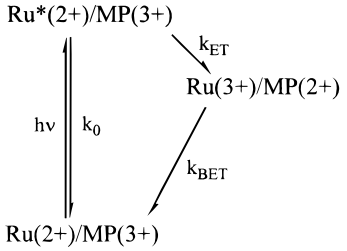

Figure 7. Proposed photochemical cycle of RuMP-11.

observed in control experiments utilizing only acMP-11. Moreover, the observed ET must be intramolecular in nature since imidazole-bound RuMP-11 shows no tendency for aggregation under the experimental conditions.

In view of the compelling experimental evidence for rapid (submicrosecond) electron transfer from the photoexcited $Ru(bpy)_3^{2+}$ derivative to the ferric heme, a simple reversible photocycle similar to the intramolecular part of the photochemical scheme in the previous article can be envisioned (Figure 7). This photocycle can be used as a model to extract estimates of k_{ET} from static luminescence quenching measurements. If the lifetimes of the intrinsic decays are known, the electron transfer rate can be calculated from the relative intensity of the luminescence according to[18]

$$\frac{I_0}{I} = \frac{\Phi_0}{\Phi} = k_{ET}\tau_0 + 1$$

where I_0, Φ_0, and τ_0 represent the intrinsic intensity, quantum yield, and lifetime of the $Ru(bpy)_3^{2+}$ analog attached to RuProHis (see previous article), I and Φ represent the measured intensity and quantum yield of RuMP-11. Since the Ru complexes have essentially the same chemical structure, the τ_0 values of the attached $Ru(bpy)_3^{2+}$ for RuMP-11 and RuProHis can be assumed to be nearly the same ($\sim$470 ns). The relative luminescence intensities normalized to the absorbance at 288 nm for RuProHis and RuMP-11 are 7778 and 717, respectively (data not shown). The forward electron transfer rate is thus calculated to be $\sim 2 \times 10^7$ s^{-1}. This value is quite consistent with the transient Raman and absorption data which clearly indicate the presence of a measurable ferrous heme population at 10 and $\sim$150 ns after $Ru(bpy)_3^{2+}$ photoexcitation and thus place the forward electron transfer rate in a range of 10^7-10^8 s^{-1}.

Concluding Remarks

The results of the investigation described in this and the preceding paper show that cytochrome *c* protein fragments can be effectively ruthenated to produce well-characterized, homogeneous samples of photoactive electron transfer systems. Many of the recent physical investigations of protein-mediated electron transfer have focused on heme-containing proteins, in general, and cytochrome *c*, in particular. Since the primary structure of RuMP-11 remains similar to that of cytochrome *c*, these models offer a unique opportunity to compare results from model systems and native proteins and thus gain further insight into protein modulation of the biological ET processes. The initial synthesis and characterization of RuMP-11 set the stage for a

(18) (a) Turro, N. J. *Modern Molecular Photochemistry*; Benjamin/Cummings: Amsterdam, 1978. (b) Sessler, J. L.; Capuano, V. L.; Kubo, Y.; Johnson, M. R.; Magda, D. J.; Harriman, A. H. In *Photoprocesses in Transition Metal Complexes, Biosystems and Other Molecules*; Kochanski, E., Ed.; Kluwer Academic Publishers: Boston, MA, 1991.

series of more quantitative investigations concerning the molecular bases for long-range ET in peptide-based systems.

The protocols described here can easily be extended to other microperoxidase species (most notably, the eight and nine amino acid forms). All three heme peptides have one or two free amino groups for forming amide bonds with carboxylic groups. Thus, model systems for photoinitiated ET can be constructed by direct covalent attachment of $Ru(bpy)_3^{2+}$ analogs containing a single acid group to the amino acids on the heme peptides. Depending on the modification position, different heme−ruthenium donor/acceptor separations can be achieved. This offers the possibility of studying the dependence of k_{ET} on donor/acceptor separation while all the other ET factors are kept constant. In this respect, these complexes are similar to the peptide/MP complexes described in the preceding article. However, the direct covalent attachment of $Ru(bpy)_3^{2+}$ analogs to the MP produces a homogeneous sample, circumventing the difficulties with sample heterogeneity posed by the equilibrium binding of the photoactive donor to the heme.

In the RuMP-11 system, the ruthenium group is attached to the microperoxidase side chain amino groups, leaving the sixth coordination site of the heme still vacant. This is potentially useful in several different ways. For instance, the heme redox potential can be manipulated by the ligation state. For example, heme octapeptide has a reduction potential of −207 mV in its five-coordinate form, but upon methionine ligation, the reduction potential shifts to −50 mV.[19] This behavior offers a unique way to vary the driving force of the system without substantially altering other parameters. Also, the spin state of the heme can be altered by using different exogenous ligands. The sixth coordination site is readily accessible to a variety of external ligands like CN^-, imidazole, Cl^-, F^-, NO, CO, etc. Because of differences in their field strengths, these ligands produce different heme spin/ligation states. Thus direct ruthenation of MPs can be used to systematically study the effects of the heme electronic state upon the ET process. This potential for spin-state variability is particularly interesting since few other systems can be manipulated to isolate and examine the effect of this parameter.

All of the above investigations are currently being pursued in our laboratory.

Acknowledgment. This work was supported by the NIH (Grant GM33330 to M.R.O.), DOE (Contract DE-AC04-94AL85000 to J.A.S.), and the Department of Energy Distinguished Postdoctoral Program (M.C.S.). We also acknowledge the assistance of the Cancer Center Protein Core Facility of the University of New Mexico.

IC970040C

(19) Moore, R. M.; Pettigrew, G. W. *Cytochrome c, Evolutionary, Structural and Physiological Aspects*; Springer-Verlag: New York, 1990.